



HAL
open science

Revealing a Vacancy Analog of the Crowdion Interstitial in Simple Cubic Crystals

B. van Der Meer, R. van Damme, M. Dijkstra, F. Smalenburg, L. Filion

► **To cite this version:**

B. van Der Meer, R. van Damme, M. Dijkstra, F. Smalenburg, L. Filion. Revealing a Vacancy Analog of the Crowdion Interstitial in Simple Cubic Crystals. *Physical Review Letters*, 2018, 121 (25), pp.258001. 10.1103/PhysRevLett.121.258001 . hal-02391107

HAL Id: hal-02391107

<https://hal.science/hal-02391107>

Submitted on 25 Mar 2024

HAL is a multi-disciplinary open access archive for the deposit and dissemination of scientific research documents, whether they are published or not. The documents may come from teaching and research institutions in France or abroad, or from public or private research centers.

L'archive ouverte pluridisciplinaire **HAL**, est destinée au dépôt et à la diffusion de documents scientifiques de niveau recherche, publiés ou non, émanant des établissements d'enseignement et de recherche français ou étrangers, des laboratoires publics ou privés.

Revealing a vacancy analogue of the crowdion interstitial in simple cubic crystals

B. van der Meer,¹ R. van Damme,¹ M. Dijkstra,¹ F. Smalenburg,² and L. Filion¹

¹*Soft Condensed Matter, Debye Institute for Nanomaterials Science, Utrecht University, Princetonplein 5, 3584 CC Utrecht, The Netherlands*

²*Laboratoire de Physique des Solides, CNRS, Univ. Paris-Sud, Univ. Paris-Saclay, 91405 Orsay, France*

(Dated: March 25, 2024)

Vacancies in simple cubic crystals of hard cubes are known to delocalize over one-dimensional chains of several lattice sites. Here, we use computer simulations to examine the structure and dynamics of vacancies in simple cubic crystals formed by hard cubes, right rhombic prisms (slanted cubes), truncated cubes and particles interacting via a soft isotropic pair potential. We show that these vacancies form a vacancy analogue of the crowdion interstitial, generating a strain field which follows a soliton solution of the sine-Gordon equation, and diffusing via a persistent random walk. Surprisingly, we find that the structure of these “voidions” is not significantly affected by changes in density, vacancy concentration, and even particle interaction. We explain this structure quantitatively using a one-dimensional model that includes the free-energy barrier particles have to overcome to slide between lattice sites and the effective pair interaction along this line. We argue that voidions are a robust phenomenon in systems of repulsive particles forming simple cubic crystals.

Many material properties of crystals are determined by the formation and diffusion of small collections of point defects inside the lattice. In crystals consisting of spherical particles, these point defects are typically fairly localized, primarily affecting the location of only a few particles, and diffuse inside the crystal through hopping motions. Therefore, imagining a point defect as localized to one specific lattice point is fundamentally correct in many cases, and forms a crucial ingredient in theories of solid-state self-diffusion [1].

However, in some cases point defects take on forms that are significantly extended in space, such as the interstitial crowdion, which was proposed by Paneth in the 1950s [2], and explored in multiple atomic crystals [3–6]. In a crowdion, the lattice distortion due to the interstitial particle is largely one-dimensional, displacing particles in a chain along a specific lattice direction, which can extend over a large number of lattice sites. Such defects have been shown to exhibit fundamentally different diffusion properties compared to their localized counterparts [6, 7], and have triggered the formulation of simple models that can capture their essential traits [8–12]. Specifically, one interesting trait of the crowdion defect is that the displacements of the particles in the defect are essentially one-dimensional and can be accurately captured by the Frenkel-Kontorova model [8, 12], which in the continuum limit reduces to the sine-Gordon equation. Recent experimental work has hinted that a vacancy-equivalent of this extended configuration, called an “anti-crowdion” [9] or a “voidion” [13], may exist in metals, where $N - 1$ particles are spread over N lattice sites in a chain [13]. However, as the atomic structure around these extended defects is typically not accessible in experiments it remains unclear whether these voidions exist, and to what extent they are related to crowdions.

Hard colloidal particles with different shapes have

emerged as an excellent model system for exploring crystalline phase behavior (e.g. [14–36]). An intriguing family of such colloidal model systems was shown to form crystals containing extended vacancy defects [32–34]. Although particles in this family have a variety of shapes and symmetries, including cubes, truncated cubes, and right rhombic prisms (“slanted cubes”), they are all predicted to form a simple cubic crystal phase with an abnormally high defect concentration, orders of magnitude higher than that of the archetypical hard-sphere crystal [37]. Experimentally, these delocalized defects have indeed been observed directly in crystals of (almost hard) cubic gold nanoparticles [35]. The presence of these defects has a profound effect on the crystal dynamics close to melting, resulting in self-diffusion rates as high as 30% of those in the corresponding fluid [32]. Both the delocalization and high diffusivity of these vacancies are strongly reminiscent of crowdion interstitials, suggesting that they may be a direct realization of the hypothesized voidion.

To test this hypothesis, we use computer simulations to examine the structure and dynamics of point defects in simple cubic crystals formed by hard cubes, slanted cubes, truncated cubes and particles interacting via a soft isotropic pair potential. We show that both vacancies and interstitials are characterized by a strain field closely following a soliton solution of the sine-Gordon equation and that the dynamics of the vacancies are well-described by a persistent random walk, similar to that seen in crowdions [6, 7, 12]. We then show that the structure of the vacancies can be explained quantitatively by considering the free-energy barrier particles have to overcome to slide between lattice sites. Surprisingly, our results demonstrate that this structure is not significantly affected by changes in density, vacancy concentration, and even particle interaction. Moreover, as we observe these defects in all the simple cubic crystals of repulsive particles we

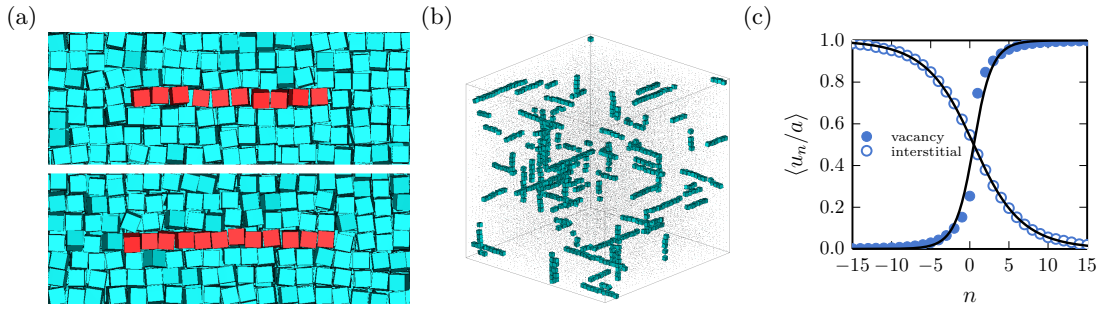


FIG. 1: (a) Typical local structure of a vacancy in a crystal of hard cubes at packing fraction $\phi = 0.65$ (top) and an interstitial at $\phi = 0.60$ (bottom) delocalized over a chain of particles. Particles which are part of the defect are colored red. (b) Tracking results revealing the position, direction and length of extended vacancies in a crystal of hard cubes at $\phi = 0.65$. Particles which are part of a vacancy are shown at their actual size while the other particles are shown much smaller. (c) Averaged displacement field along the vacancy (solid markers) and the interstitial (open marker) for a hard-cube system at $\phi = 0.60$. The displacements inside these defects follow the soliton solution to the sine-Gordon equation (black lines).

have investigated - ranging from hard anisotropic particles to a much longer ranged soft isotropic potential - we argue that voidions are a robust phenomenon in systems of repulsive particles forming simple cubic crystals.

We begin our investigation by characterizing the displacement field of particles around defects in equilibrium crystals of hard cubes (i.e. overlaps between particles are not allowed), with edge length σ . We perform Monte Carlo (MC) and event-driven molecular dynamics (EDMD) simulations [32, 38, 39] of three-dimensional crystals of N particles. Each simulation is initialized as a perfect crystal containing its net equilibrium concentration of vacancies $\alpha = (N_L - N)/N_L$, where N_L is the number of lattice sites. Note that in principle, additional vacancy-interstitial pairs can form which increase the total number of vacancies. The net equilibrium vacancy concentration for each crystal density is taken from previous free-energy calculations presented in Refs. 32 and 34. In each simulation, we track the defects, their length, and their orientation by examining the occupancy of Wigner-Seitz cells in the crystal (see Supplemental Information (SI) [40]). Examples of a vacancy and an interstitial are shown in Fig. 1(a). Clearly in both cases, the defect is extended over a long chain of lattice sites. Note that the number of vacancies is much larger than the number of interstitials in these systems. To provide a better image of the distribution of defects in a crystal, Fig. 1(b) shows all vacancies in a typical crystal of hard cubes, illustrating that the defects are delocalized with random positions and orientations along the three crystal axes. Interestingly, as shown in the SI [40] and discussed briefly in Ref. 32, despite the high concentration of these defects, they essentially do not interact.

In order to characterize the structure of the defects, we measure the average particle displacements $u_n = x_n - an$ around vacancies and interstitials, along the defect direction, where x_n is the position of particle n along the defect, and a is the crystal lattice spacing. We choose $n = 0$

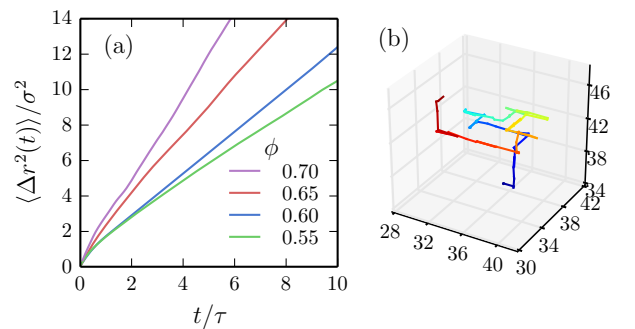


FIG. 2: (a) Mean squared displacement of the center of the vacancies for the hard-cube system at different packing fractions. (b) Trajectory of the center of a vacancy in the hard-cube system at a packing fraction $\phi = 0.65$.

to correspond to the particle just before the defect center and use “standard” boundary conditions: $u_{n=-\infty} = a$, $u_{n=\infty} = 0$ for the interstitial and $u_{n=-\infty} = 0$, $u_{n=\infty} = a$ for the vacancy. We plot these displacement fields for a system of hard cubes at packing fraction $\phi = 0.60$ in Fig. 1(c), where $\phi = Nv_0/V$ with v_0 the volume of the particle and V the volume of the system. From these displacement fields we see that the vacancies affect the behaviour of about 10 particles on average, while for the interstitials, it is closer to 20.

One important characteristic of a crowdion defect is that the displacements of the particles in the defect are essentially one-dimensional and can be well described by the Frenkel-Kontorova model [8, 12]. Hence, to determine whether the defects are realizations of crowdions and voidions, we compare our results to the soliton solution of the sine-Gordon equation (black lines), i.e. the continuum limit of the Frenkel-Kontorova model using a single fitting parameter to match the extension of the defect (see SI [40]). As Fig. 1(c) shows, we observe excellent agreement for the interstitial defects and good agreement for the vacancy defects, indicating that at least the

structure of the defects is consistent with crowdions and voidions. This is somewhat surprising, since the classic Frenkel-Kontorova model assumes harmonically interacting particles in a periodic sinusoidal potential, while the interactions between hard cubes are strongly anharmonic.

As vacancies are the predominant type of defect in these crystals, in the rest of this Letter we focus purely on the voidions.

To further confirm that the vacancies are indeed well-identified as voidions, we now turn our attention to their dynamics using EDMD simulations. In Fig. 2(a), we plot the mean squared displacement as a function of time for the center of the vacancies in crystals of hard cubes at their equilibrium vacancy concentration. Here our time unit is $\tau = \sqrt{\beta m \sigma^2}$, where m is the mass of a particle and $\beta = 1/k_B T$ with k_B Boltzmann's constant and T the temperature. Counter-intuitively, the vacancy diffusivity goes up with increasing packing fraction in contrast to vacancy diffusion in most systems, where the diffusivity goes down drastically with increasing packing fraction (e.g. Ref. 41). A typical trajectory of such a defect is shown in Fig. 2(b). Clearly, the vacancy diffuses by gliding along the main crystalline lattice directions, and from time to time, by reorienting. The gliding process itself requires very little activation energy, requiring only very small displacements of each particle in the defect. Reorienting, on the other hand, requires the vacancy to shrink to a single lattice site, and then regrow in a new direction. This is an activated process that occurs on time scales much slower than the gliding diffusion, resulting in a persistent random walk as seen in crowdions [6, 7, 12].

The diffusion in this system is thus governed by two separate time scales: the one-dimensional diffusion, and the time scale associated with reorientations. Interestingly, as shown in the SI [40], the reorientation time increases with packing fraction, implying that the defects glide for longer along the same axis and resulting in a faster overall diffusion. Note that since the equilibrium defect concentration decreases rapidly with packing fraction [32], the total self-diffusivity of the particles in the crystal still slows down with increasing packing fraction.

In summary, the vacancies observed in the simple cubic crystals of hard cubes clearly show strong similarities to crowdions in atomic systems, both in terms of structure and diffusive behavior. Hence, we identify these vacancies as a vacancy-analogue of crowdions: voidions.

To determine the robustness of these defects in simple cubic lattices, we use MC and EDMD simulations in the canonical ensemble to explore three additional model systems for repulsive particles that form simple cubic lattices, namely slanted cubes with a slant angle $\theta = 72.5^\circ$ [34], truncated cubes [33] (see SI [40]), and a soft isotropic repulsive pair interaction (ISO), introduced in Refs. 42, 43. A model of the slanted cube and

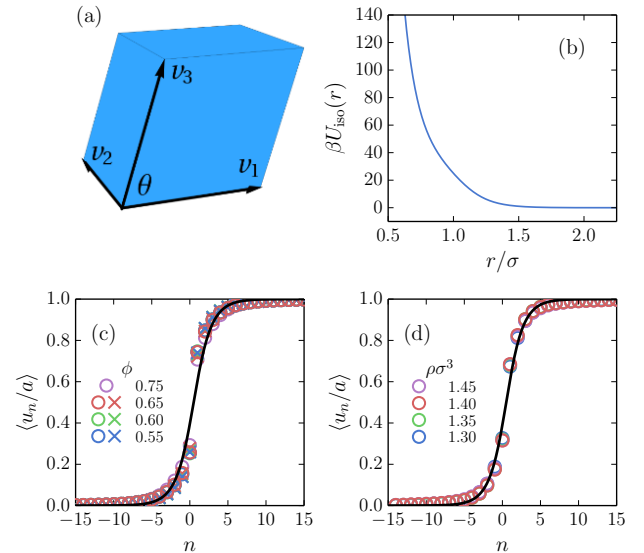


FIG. 3: (a) Model of a slanted cube with slant angle $\theta = 72.5^\circ$. The vectors spanning the shape are given by $\mathbf{v}_1 = \{\sigma, 0, 0\}$, $\mathbf{v}_2 = \{0, \sigma, 0\}$, and $\mathbf{v}_3 = \{\sigma \cos \theta, 0, \sigma \sin \theta\}$. (b) Plot of the soft isotropic interaction potential from Refs. 42, 43. Note that here σ is an arbitrary length unit. (c) Averaged displacement field along the vacancy at different ϕ for cubes (circles) and slanted cubes (crosses). (d) Averaged displacement field along the vacancy for a simple cubic crystal of spheres interacting through the isotropic potential shown in (b), for different densities. The black lines in (c, d) correspond to fitting the data to the soliton solution to the sine-Gordon equation.

the ISO pair interaction are shown in Figs. 3(a) and (b), respectively. In Fig. 3(c), we plot the average displacement field around a vacancy for both cubes and slanted cubes (with slant angle $\theta = 72.5^\circ$) at several packing fractions. Surprisingly, the displacement fields for the different packing fractions ϕ and for the two particle shapes collapse onto a single curve when the displacements are normalized with respect to the lattice spacing a . Furthermore, in Fig. 3(d), we plot the same displacement fields for the ISO potential, at several number densities in the regime where the simple cubic lattice is stable. We again observe a similar defect-shape, which is independent of the density. A similar result for truncated cubes is shown in the SI [40]. In all cases, the displacement fields suggest an average length of vacancies of around 10 particles.

In order to understand the mechanism which controls the length of these defects, we draw inspiration from the Frenkel-Kontorova model and consider our defect as a one-dimensional row of particles, which experiences an effective periodic potential due to the rest of the crystal. However, instead of assuming harmonically interacting particles in a sinusoidal potential, we use the true particle interactions and measure the effective free-energy landscape. To measure this effective potential, we perform Monte Carlo simulations of defect-free crystals where a

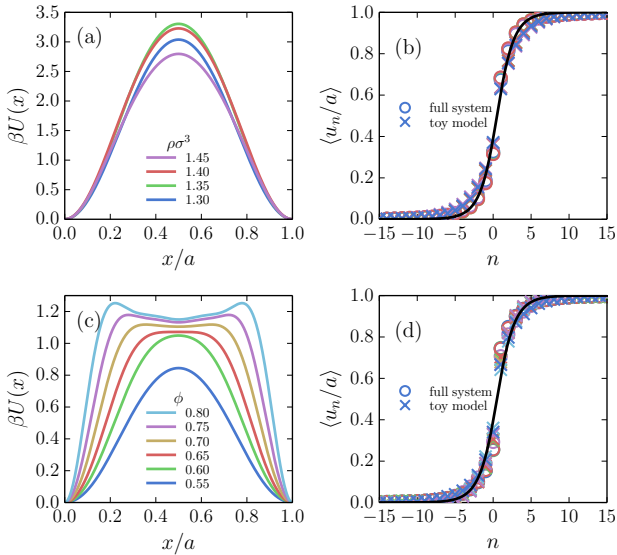


FIG. 4: (a) Free-energy barriers $U(x)$ for the ISO system at different densities. (b) The resulting displacement fields obtained by single-row simulations for a vacancy using these free-energy barriers (crosses), compared to the displacement fields as measured in the full system (circles). (c,d) Free-energy barriers and displacement fields for the hard-cube system. In (b, d) colors are the same as in (a, c). The black lines in (b, d) correspond to fitting the data to the soliton solution to the sine-Gordon equation.

single row of particles is subject to an additional external periodic potential $V(x)$, where x is measured along the axis of the chosen row. This potential is then tuned (see SI [40]) until the density profile $\rho(x)$ along the row is constant, indicating that the imposed external potential exactly cancels out the effects of the rest of the crystal on the particle positions along the row. Hence, the particles in the row experience an effective potential $U(x) = -V(x)$ from the rest of the crystal, on top of the interactions experienced between particles within the row.

We plot $U(x)$ for several number densities of the ISO system in Fig. 4(a). In all cases, $U(x)$ shows a clear minimum at $x = 0$, corresponding to the equilibrium lattice position, and a peak at $x = a/2$, representing a free-energy barrier inhibiting sliding between lattice sites. We now impose the measured potentials $U(x)$ to simulate a simplified model of the defect by fixing a row of particles (interacting via the ISO interaction) along the x -axis with a single vacancy, and we again measure the displacement field around the defect. The resulting displacement fields are compared to those measured in the full crystal in Fig. 4(b), showing excellent agreement for all densities. Note that the agreement at different densities is not trivial, as both the strength of $U(x)$ and the spacing between the particles (and hence their interaction strength) are density-dependent (see SI [40]).

We repeat this procedure for the system of hard cubes, and show the effective free-energy barrier $U(x)$ in Fig. 4(c). In comparison to the isotropic potential, the barrier shape for cubes is significantly more complex, with the top of the barrier flattening and even showing a secondary minimum at high packing fractions. In this case, simulating a one-dimensional system using $U(x)$ is complicated by the presence of rotational degrees of freedom, which are inhibited by interactions with the rest of the crystal. To approximate this, we simulate cubes confined in a mean-field square “tunnel” consisting of four hard walls at a distance set by the lattice constant (see SI [40]). Within this approximation, we again find excellent agreement for the displacement field around a vacancy, as shown in Fig. 4(d). Note that including the rotational degrees of freedom is essential in order to capture the correct vacancy length and shape.

This toy model clearly shows that the vacancy displacement fields arise from a subtle competition between the free-energy barriers and effective interparticle repulsions. Specifically, the density-independent displacement field in the cubes can be explained by an increase in barrier height and width as a function of density, which is compensated by a stronger inter-particle repulsion due to the smaller lattice spacing. As shown in the SI [40], increased particle alignment also affects the effective repulsion, but is dominated by the effects of the lattice spacing. Similarly, in comparison to the cubes, the ISO system has much higher barriers, but also much stronger effective repulsions, resulting in a similar defect length. What remains a mystery, however, is why in each case of repulsive particles forming simple cubic crystals studied so far, this competition serendipitously results in essentially the same displacement field – with a length of approximately 10 particles – almost entirely independent of interaction, particle shape, and density.

The dependence of the defect structure on the competition between the free-energy barriers and the interparticle repulsions hints at a reason we observe these defects in simple cubic crystals of hard particles, and not in more highly coordinated lattices like face-centered-cubic crystals. Specifically, on lattices with low coordination numbers, the number of particles contributing to the barrier is low, resulting in lower barriers in comparison to the interparticle interactions. Moreover, this mechanism also explains why such defects have not been observed more frequently: in attractive systems, which are more commonly found in nature, the attractions can both increase the barrier and remove the repulsions necessary to have the particles spread along the rows. Indeed, attractive interactions have been demonstrated to strongly suppress vacancy delocalization in simple cubic crystals of cubic nanoparticles [44]. Hence, the attractions in such systems need to be tuned to be weak in order to observe delocalized vacancies [35].

In conclusion, we have demonstrated the existence of

voidions in simple cubic crystals formed by a range of repulsive potentials, and in fact, every repulsive potential we have examined shows stunningly similar vacancy structures that are essentially density independent. We have also elucidated a mechanism which accurately captures the extension of the vacancies, demonstrating that the length of the vacancies is controlled by a complex interplay between (low) free-energy barriers in rows of particles, and the particle interactions. Our results clearly demonstrate that voidions are a common property of simple cubic lattices of repulsive particles.

We acknowledge funding from the Dutch Sector Plan Physics and Chemistry, and funding from a NWO-Veni grant (NWO-VENI grant No. 680.47.432). We would like to thank Michiel Hermes, Matthieu Marechal, Hartmut Löwen, and Jette van den Broeke for useful discussions.

-
- [1] H. Mehrer, *Diffusion in solids: fundamentals, methods, materials, diffusion-controlled processes* (Springer Science & Business Media, Berlin, 2007), Vol. 155.
- [2] H. R. Paneth, *Physical Review* **80**, 708 (1950).
- [3] S. Han *et al.*, *Phys. Rev. B* **66**, 220101 (2002).
- [4] Y. N. Osetsky *et al.*, *Philos. Mag.* **83**, 61 (2003).
- [5] D. Nguyen-Manh, A. Horsfield, and S. Dudarev, *Phys. Rev. B* **73**, 020101 (2006).
- [6] P. M. Derlet, D. Nguyen-Manh, and S. Dudarev, *Phys. Rev. B* **76**, 054107 (2007).
- [7] L. A. Zepeda-Ruiz *et al.*, *Phys. Rev. B* **70**, 060102 (2004).
- [8] T. Kontorova and J. Frenkel, *Zh. Eksp. Teor. Fiz.* **8**, 1340 (1938).
- [9] A. Landau, A. Kovalev, and A. Kondratyuk, *Phys. Status Solidi B* **179**, 373 (1993).
- [10] A. Kovalev, A. Kondratyuk, A. Kosevich, and A. Landau, *Phys. Status Solidi B* **177**, 117 (1993).
- [11] O. M. Braun and Y. S. Kivshar, *Phys. Rep.* **306**, 1 (1998).
- [12] S. Dudarev†, *Philos. Mag.* **83**, 3577 (2003).
- [13] Y. Matsukawa and S. J. Zinkle, *Science* **318**, 959 (2007).
- [14] D. Frenkel and A. J. Ladd, *J. Chem. Phys.* **81**, 3188 (1984).
- [15] P. Bolhuis and D. Frenkel, *J. Chem. Phys.* **106**, 666 (1997).
- [16] C. Vega and P. A. Monson, *J. Chem. Phys.* **107**, 2696 (1997).
- [17] S. Auer and D. Frenkel, *Nature* **409**, 1020 (2001).
- [18] E. Zaccarelli *et al.*, *Phys. Rev. Lett.* **103**, 135704 (2009).
- [19] P. F. Damasceno, M. Engel, and S. C. Glotzer, *Science* **337**, 453 (2012).
- [20] A. Haji-Akbari *et al.*, *Nature* **462**, 773 (2009).
- [21] A. L. Thorneywork, J. L. Abbott, D. G. Aarts, and R. P. Dullens, *Phys. Rev. Lett.* **118**, 158001 (2017).
- [22] F. A. Lavergne, D. G. Aarts, and R. P. Dullens, *Phys. Rev. X* **7**, 041064 (2017).
- [23] S. Torquato and Y. Jiao, *Phys. Rev. E* **80**, 041104 (2009).
- [24] S. Torquato and Y. Jiao, *Nature* **460**, 876 (2009).
- [25] R. D. Batten, F. H. Stillinger, and S. Torquato, *Phys. Rev. E* **81**, 061105 (2010).
- [26] U. Agarwal and F. A. Escobedo, *Nat. Mater.* **10**, 230 (2011).
- [27] R. Ni *et al.*, *Soft Matter* **8**, 8826 (2012).
- [28] M. Dijkstra, *Adv. Chem. Phys.* **35** (2014).
- [29] S. Dussi and M. Dijkstra, *Nat. Commun.* **7**, 11175 (2016).
- [30] N. Tasios and M. Dijkstra, *J. Chem. Phys.* **146**, 144901 (2017).
- [31] J.-M. Meijer *et al.*, *Nat. Commun.* **8**, 14352 (2017).
- [32] F. Smalenburg, L. Filion, M. Marechal, and M. Dijkstra, *Proc. Natl. Acad. Sci. USA* **109**, 17886 (2012).
- [33] A. P. Gantapara, J. de Graaf, R. van Roij, and M. Dijkstra, *Phys. Rev. Lett.* **111**, 015501 (2013).
- [34] R. van Damme *et al.*, *J. Chem. Phys.* **147**, 124501 (2017).
- [35] J. Gong *et al.*, *Nat. Commun.* **8**, 14038 (2017).
- [36] A. K. Sharma and F. A. Escobedo, *J. Phys. Chem. B* **122**, 9264 (2018).
- [37] S. Pronk and D. Frenkel, *J. Phys. Chem. B* **105**, 6722 (2001).
- [38] B. J. Alder and T. E. Wainwright, *J. Chem. Phys.* **31**, 459 (1959).
- [39] L. Hernández de la Peña, R. van Zon, J. Schofield, and S. B. Opps, *J. Chem. Phys.* **126**, 074105 (2007).
- [40] Supplemental material (link here) .
- [41] B. van der Meer, M. Dijkstra, and L. Filion, *J. Chem. Phys.* **146**, 244905 (2017).
- [42] A. Jain, J. R. Errington, and T. M. Truskett, *Soft Matter* **9**, 3866 (2013).
- [43] A. Jain, J. R. Errington, and T. M. Truskett, *J. Chem. Phys.* **139**, 141102 (2013).
- [44] J. S. van der Burgt *et al.*, *J. Phys. Chem. C* **122**, 15706 (2018).